LANGMUIR Article
Cite This: Langmuir 2017, 33, 12260-12266 pubs.acs.org/Langmuir

Clustering and Percolation in Suspensions of Carbon Black

Jeffrey J. Richards,*[,†] Julie B. Hipp,[‡] John K. Riley,[†] Norman J. Wagner,[‡] and Paul D. Butler[†]

[†]NIST Center for Neutron Research, National Institute of Standards and Technology, Gaithersburg, Maryland 20899, United States
[‡]Department of Chemical and Biomolecular Engineering, University of Delaware, Newark, Delaware 19716, United States

Supporting Information

ABSTRACT: High-structured carbon fillers are ubiquitous as the conductive additive comprising suspension-based electrochemical energy storage technologies. Carbon black networks provide the necessary electrical conductivity as well as mechanical percolation in the form of a yield stress. Despite their critical role in determining system performance, a full mechanistic understanding of the relationship between the electrical transport characteristics of the percolated, conductive networks of carbon black, and the rheological properties is lacking, which hinders the rational design and optimization of flowable electrodes and the processing of electrolytes for batteries. Here, we report on the microstructural origin of the rheological and electrical properties of two commonly used conductive additives in neat propylene carbonate. From quiescent mechanical and structural studies, we find that the gelation of these carbon black suspensions is best described by the dynamic arrest of a clustered fluid phase. In contrast, the temperature and frequency dependence of the ac conductivity near this transition shows that mesoscale charge transport is determined by hopping between localized states that does not require a stress-bearing network. This unique combination of microstructural characterization with rheological and electrical measurements enables testing prevailing theories of the connection between electrical and mechanical percolation as well as improving conductive additives to enhance electrochemical performance.

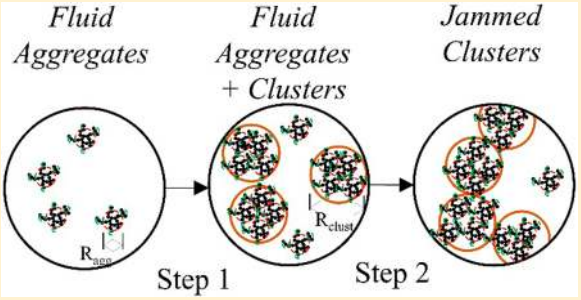

INTRODUCTION

The formation of stress-bearing, interconnected particle networks is responsible for the liquid−solid transition in a wide variety of attractive colloidal suspensions. This so-called jamming transition demarcates the boundary between a suspension that is liquid-like and solid-like and is often characterized macroscopically by the divergence of the zero-shear viscosity and onset of a finite yield stress and elastic modulus.[1] At a critical volume fraction, ϕ, or attraction strength, U, properties typical of critical behavior are observed. On microscopic length scales, this transition is characterized by the dynamic arrest of the particles that comprise the network. Polymer−colloid mixtures comprise the bulk of the experimental and theoretical work to date exploring the origins of phase behavior, gelation characteristics, and dynamical arrest.[2,3] The physical insights gleaned through these efforts provide a stepping stone to understanding more complex colloidal systems that are typically used in important technological applications, such as carbon black suspensions. A renewed interest in the fluid−solid transition in carbon black suspensions is motivated by their use as conductive additives in flowable electrochemical slurries.[4−6] In these suspension electrodes, the electrical conductivity, yield stress, and viscosity are key design parameters for achieving performance parity with other electrochemical technologies.[7] Despite their widespread use, there's a fundamental lack of experimental data, and hence understanding, of the relationship between the electrical and rheological characteristics of carbon black suspensions and their microstructure.

A common hypothesis in the literature is that the network backbone bearing stress in colloidal gels of carbon black is the same percolated network that conducts electrical charge across the sample.[8] The implications of this hypothesis are an intrinsic coupling between the elastic and electrical properties through the topology and number density of stress-bearing chains and that a system-spanning network of contacts must be present for electrical conduction to occur. However, Narayanan et al. have recently attributed electrical transport in carbon black gels to hopping, which would not necessarily require a stress-bearing network for conduction.[9] A detailed study on the role of microstructure to the overall conductivity of these system-spanning networks has not been experimentally elucidated, and therefore, their role in determining electrical performance remains unclear. In this work, we report measurements of the electrical and rheological properties of two model, conductive additives formulated from commercially available, high-structured carbon blacks. We characterize the electrical and rheological properties of suspensions formed in propylene carbonate at volume fractions spanning the gel boundary and find that the stress-bearing structures are not responsible for the bulk of electrical charge transport. Instead, we conclude that

Received: July 21, 2017
Revised: September 26, 2017
Published: October 2, 2017

DOI: 10.1021/acs.langmuir.7b02538
Langmuir 2017, 33, 12260−12266

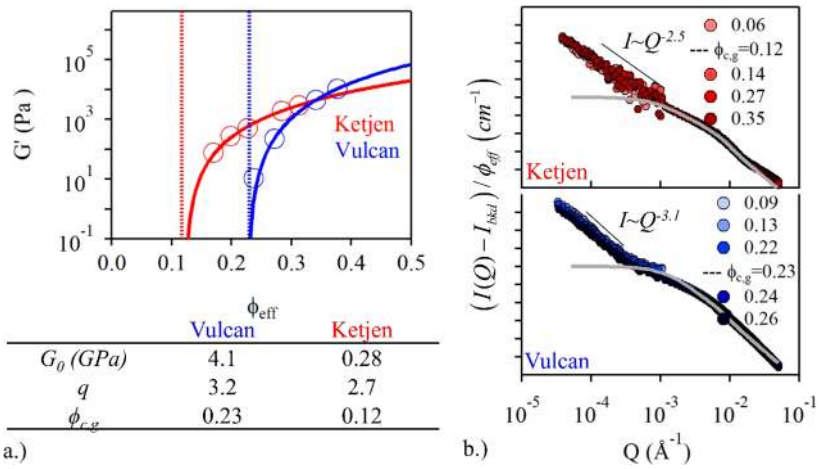

	Vulcan	Ketjen
G_0 (GPa)	4.1	0.28
q	3.2	2.7
$\phi_{c,g}$	0.23	0.12

Figure 1. (a, Top) Elastic modulus, G', as a function of normalized volume fraction, ϕ_{eff}, for Ketjen and Vulcan gels. The torque resolution using this tooling is ~0.1 Pa. The model fits to the elastic moduli are overlaid on the data points. (a, bottom) Table of fit parameters to percolation equation, $G' = G_0(\phi_{eff} - \phi_{c,g})^q$. (b) Normalized combined desmeared USANS and SANS intensity, $I(Q)$, versus scattering wave vector, Q, for Ketjen (top) and Vulcan (bottom) above and below mechanical percolation threshold. The solid black lines indicate the power-law slope value at low Q, and the solid gray lines are the form-factor model fits described in the Supporting Information for the dilute carbon black suspensions. Volume fractions that are specified correspond to ϕ_{eff}.

hopping transport between carbon clusters dominates the temperature and frequency dependence of the ac conductivity even when stress-bearing bonds are present. Finally, we connect these macroscopic observations to the microscopic picture using small angle neutron and light scattering measurements.

EXPERIMENTAL SECTION

Vulcan XC-72 (Cabot Corp.) and KetjenBlack EC-600JD (AkzoNobel) were suspended in neat propylene carbonate (Aldrich). The solvent has a dielectric constant of $\varepsilon_m = 64$ and viscosity of $\eta_m = 2.5$ mPa·s. Suspensions of carbon black are prepared using a Silverson L4RT high-shear homogenizer to ensure that all the carbon is fully suspended and wetted by propylene carbonate. Under significant dilution, the carbon black particles are colloidally stable with Vulcan and Ketjen possessing a R_H = 135 and 167 nm, respectively (Supporting Information). Rheological testing was performed on a TA Instruments ARES-G2 rheometer using a 40 mm cone and plate stainless steel geometry with 1° cone angle. A preshear protocol was employed to ensure consistency of the rheological measurements. Suspensions were presheared by 20 consecutive 30 s long flow ramps from 500 to 0.1 1/s followed by a resting period of 20 min with no applied shear. This protocol was chosen to reduce any residual effects the high-shear homogenization preparation protocol may have on the rheology.[10] The measurements were performed at 25 °C in the linear regime (γ_0 = 0.001) as a function of frequency (Supporting Information Figure S.1). SANS measurements were performed on the NG7 30 m small angle neutron scattering (SANS) diffractometer at the NIST Center for Neutron Research in Gaithersburg, MD, USA.[26] The entire Q-range was acquired by collecting SANS profiles using four configurations, where $Q = 4\pi/\lambda \sin(\theta/2)$. Three configurations taken at λ = 6 Å with $\Delta\lambda/\lambda$ = 10% covering the Q-range from 3×10^{-3} Å^{-1} < Q < 0.4 Å^{-1}. The Q-range from 1×10^{-3} Å^{-1} < Q < 6×10^{-3} Å^{-1} was acquired at λ = 8 Å with $\Delta\lambda/\lambda$ = 10%. Ultra small angle neutron scattering (USANS) measurements were performed using the BT-5 instrument at the NIST center for Neutron Research. The accessible Q-range in this instrument is 5×10^{-5} Å^{-1} < Q < 1×10^{-3} Å^{-1}, and the incident beam is slit collimated. For the SANS and USANS experiments, the samples were presheared in the rheometer using identical protocols as for the rheological experiments before loading into titanium cells with quartz windows and 1 mm path length for both the SANS and USANS measurements. The scattering data were reduced to absolute scale using standard procedures and IGOR Pro reduction macros.[11] Dielectric spectroscopy measurements were made using a network analyzer (Agilent 4294A-1D5) with a frequency range spanning 40 Hz to 100 MHz in a sealed cell with stainless steel electrodes using a 1.5 mm Teflon spacer and 100 mV voltage amplitude.[12] Short-circuit and open measurements were made and the measured data corrected.[13] Dynamic light scattering (DLS) measurements were made with a Brookhaven Instruments Corp. ZetaPALS particle sizer after diluting samples to 1.0×10^{-5} weight fraction in neat propylene carbonate. Transmission electron microscopy (TEM) measurements were made using a JEM-2010F transmission electron microscope supported on Electron Microscopy Sciences Formvar/Carbon 200 mesh copper grids. The size and number density of primary carbon particles were counted using ImageJ. Unless otherwise specified, all error bars represent one standard deviation from the reported average.

RESULTS AND DISCUSSION

Dynamic Arrest and the Stress-Bearing Network Properties. The model suspension electrodes are gels formed from two commercial, conductive carbon blacks used in battery and fuel cell applications, KetjenBlack EC-600JD (AkzoNobel) and Vulcan XC-72 (Cabot). These particles are dispersed into neat propylene carbonate using a Silverson high-shear mixer. Linear viscoelastic moduli are measured as a function of frequency for suspensions over a broad range of particle volume fraction using a low strain amplitude (γ_0 = 0.001). The liquid−solid transition is identified by the onset of a finite elastic modulus at a critical volume fraction, $\phi_{c,g}$.[14] Samples prepared below $\phi_{c,g}$ showed no measurable elasticity within the torque resolution of the rheometer and were colloidally stable for weeks on the benchtop, while above $\phi_{c,g}$ the elastic moduli are nearly independent of frequency (Figure S.1). Following the convention established for polymer−carbon composites to eliminate the differences between the level of structure (i.e., porosity) in carbon black particles,[15] the carbon volume fraction based on the dry mass, ϕ_{CB}, is rescaled for both carbon blacks by $\phi_{eff} = \phi_{CB}/\Phi_{CB,R_{agg}}$, where $\Phi_{CB,R_{agg}}$ is determined from the structural parameters of the primary aggregate described in the Supporting Information and is 0.06 and 0.20 for Ketjen and Vulcan, respectively. This rescaling allows for direct comparison between the two carbons. The elastic modulus at 1 Hz is plotted versus ϕ_{eff} in Figure 1a and fit

DOI: 10.1021/acs.langmuir.7b02538
Langmuir 2017, 33, 12260−12266

to the critical scaling law: $G' = G_0(\phi_{eff} - \phi_{c,g})^q$.[1] The fit parameters G_0, q *and* $\phi_{c,g}$ are shown in the table inset in Figure 1a for both model systems.

Microstructure Near the Liquid−Solid Transition. SANS and USANS measurements provide microstructural characterization of these suspension electrodes over a range of length scales from nanometers to micrometers. Shown in Figure 1b are the combined desmeared USANS and pinhole smeared SANS profiles for both Ketjen and Vulcan suspensions at concentrations that span $\phi_{c,g}$ identified in Figure 1a. The scattering profiles are background subtracted and normalized to ϕ_{eff}. When scaled this way, both Ketjen and Vulcan suspensions show nearly identical scattering profiles with the largest difference at high-Q originating from the core−shell nature of the primary particles that comprise the Ketjen primary aggregates (Figure S.3). Through $\phi_{c,g}$ there are no significant structural transitions evident within the Q-range investigated for either carbon black. The low-Q power-law slopes are shown in Figure 1b for both samples and are 2.5 and 3.1 for Ketjen and Vulcan, respectively. These power-law values are consistent with the presence of compact structures exceeding many micrometers in diameter.[16] To further investigate this low-Q structure, the desmeared form factor (see Supporting Information eq S.2) of the carbon black aggregates, overlaid on the scattering profiles in Figure 1b, was divided from the measured scattering data to recover the static structure factor, $S(Q)$, as shown in Figure 2a.[17] Close examination of the Vulcan scattering profiles reveals a volume fraction dependent depression for $1 < 2QR_H < 10$. This behavior is characteristic of the excluded volume interaction that is seen in spherical colloids where the well depth increases with concentration.[18] The magnitude of the low-Q structure factor determined by this normalization closely resembles measurements reported by Lu et al. for colloidal clusters in phase-separating colloid−polymer mixtures.[16] Stable colloidal clusters are observed in a variety of aggregating colloid and protein systems.[19−21]

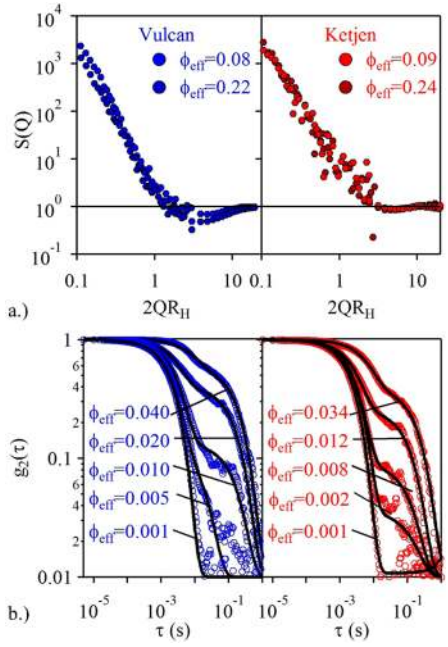

Figure 2. (a) Static structure factor, $S(Q)$, versus scattering wave vector, renormalized for the hydrodynamic diameter of the primary carbon black aggregates, $2QR_H$, for Ketjen and Vulcan fluids near the critical gel concentration. (b) Correlation functions, $g_2(\tau)$, for Vulcan and Ketjen samples equilibrated at the specified volume fractions and then diluted to 1.0×10^{-5} weight fraction to perform the measurement. The correlation functions represent the irreversible aggregation that takes place as a function of concentration. Distribution fits are overlaid as the solid black lines, and parameters from fits are specified in Supporting Information Figure S.4.

To determine whether a stable clustered fluid phase exists, a series of fluid sample concentrations below $\phi_{c,g}$ ($\phi_{eff} \sim 10^{-3}$ to 10^{-1}) were prepared for both carbon blacks. These samples were then diluted to the same concentration ($\phi_{eff} \sim 10^{-5}$) in neat propylene carbonate without any vigorous mixing or sonication for measurement of the particle size distribution by DLS. Figure 2b shows the correlation functions that result from samples of increasing concentration for both Ketjen and Vulcan. As the volume fraction is increased, the correlograms exhibit a continuous transition from a monomodal to multimodal relaxation spectrum with an additional, longer time relaxation feature. Distribution fits to the correlation functions are shown in Figure 2b, where the fitting function is the sum of two exponential functions. The first relaxation feature is associated with the hydrodynamic size of the primary carbon aggregates (Figure S.4), and we attribute the second, slower relaxation to clusters that are comprised of irreversibly bonded primary aggregates that are stable upon dilution. As the concentration is increased for both Ketjen and Vulcan, the number density of these clusters increases relative to the primary aggregate population, while the average hydrodynamic size of both populations remains relatively unchanged (see Figure S.4). While the resolution of long relaxation times is limited for DLS measurements, the hydrodynamic size corresponding to the longer relaxation time is ∼5−6 μm for both Vulcan and Ketjen. This length scale is consistent with the structural length scale apparent in the USANS measurements, although the full Guinier plateau cannot be resolved due to the instrument resolution. It is also consistent with the length scales of carbon black agglomerates commonly seen in carbon black suspensions.[22,23]

Electrical Percolation and a Mechanistic Understanding of Electrical Transport. The electrical properties of these suspensions were measured using impedance spectroscopy for volume fractions approaching $\phi_{c,g}$ (Figure S.5 and Figure S.6) over a wide frequency range (40 Hz to 40 MHz). The frequency dependence of the complex conductivity shows characteristics of both ionic and electrical transport that depend on the volume fraction of carbon black. The effect of changing carbon volume fraction on the electrical component of the spectra can be examined by plotting the ac conductivity, σ_{ac}, and relative permittivity, ε', and the relaxation time, τ, versus ϕ_{eff} for suspensions of both Ketjen and Vulcan in Figure 3. Due to the double-layer charging at the electrode−electrolyte and carbon−electrolyte interfaces, electrode polarization dominates the impedance spectra at low frequencies. The total conductivity, σ_{ac}, is therefore taken at 20 kHz to probe the macroscopic response of the free ions and electrons within the sample. This conductivity contains both the ionic, $\sigma_{i,ac}$, and electronic contributions, $\sigma_{e,ac}$, to mobile charge carriers $\sigma_{ac} = \sigma_{e,ac} + \sigma_{i,ac}$.[24] At low carbon black concentrations, σ_{ac} is a weak function of carbon black concentration and dominated by the intrinsic ionic conductivity of the neat propylene carbonate and the ions dissociated from the carbon black surface.[25] Above ϕ_{eff} = 0.005 and 0.01, respectively, both Ketjen and Vulcan show electrical percolation behavior characterized by a strong

DOI: 10.1021/acs.langmuir.7b02538
Langmuir 2017, 33, 12260−12266

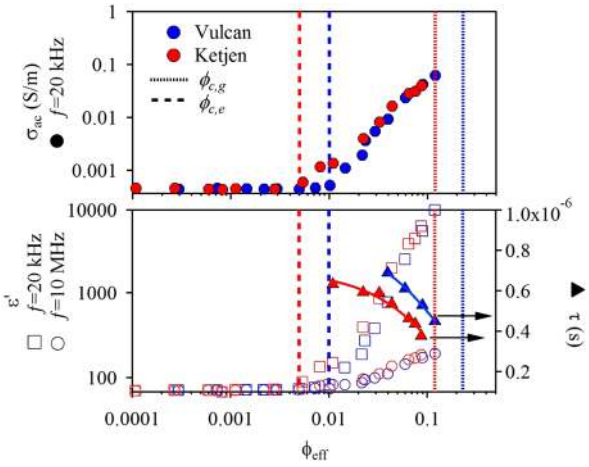

Figure 3. (Top) ac conductivity, σ_{ac} (S/m), measured at f = 20 kHz, versus effective volume fraction, ϕ_{eff}, for Vulcan and Ketjen. (Bottom) Relative permittivity, ε', measured at f = 20 kHz and f = 10 MHz, respectively, and τ versus effective volume fraction, ϕ_{eff}. Solid lines through τ are to guide the eye and the arrows to indicate axis. For reference, the mechanical percolation threshold, $\phi_{c,g}$, is indicated by the short-dashed vertical line and the electrical percolation threshold, $\phi_{c,e}$, indicated by the long-dashed vertical line for both Ketjen and Vulcan.

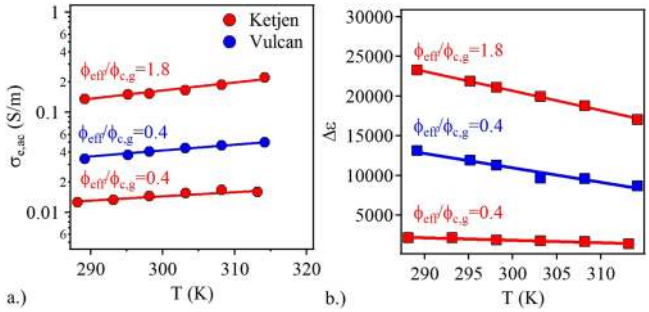

Figure 4. Temperature dependence of (a) the total conductivity, $\sigma_{e,ac}$, and (b) the relaxation strength, $\Delta\varepsilon = \varepsilon_{20kHz} - \varepsilon_{10MHz}$, for Vulcan and Ketjen samples at concentrations above and below the jamming transitions. Overlaid in panel a are model fits to the Mott equation, $\sigma_{e,ac} = \sigma_0/T^{0.5}\exp(-(T_0/T)^{0.25})$. Overlaid in panel b are linear fits to $\Delta\varepsilon$ versus T.

increase of the ac conductivity above a critical volume fraction, $\phi_{c,e}$. The samples above $\phi_{c,e}$ exhibit charge transport characteristics consistent with those measured from carbon−polymer composites where the highest conductivities achieved are far below that of the intrinsic conductivity of the carbon black powder.[26] The permittivities, ε', show a strong scaling with volume fraction above $\phi_{c,e}$ at both low and high frequencies with a strong frequency dependence (Figure S.6). Their magnitude far exceeds that of a dipolar response, is far above that of propylene carbonate, and, therefore, must arise due to electron delocalization over mesoscopic length scales. This phenomenon is known as a conduction current relaxation. Its presence is consistent with current flowing along pathways unaligned with the electric field that gives rise to a partial interfacial polarization.[27] Fits to the high-frequency ac response of the material (Supporting Information Figure S.6) using eq S.6 describe the frequency dependence of this response for all volume fractions above $\phi_{c,e}$ and also allow for an estimation of a relaxation time, τ, whose physical origin is connected to the topology of the percolated path through the Barton−Nakajima−Namikawa condition.[27]

The conduction mechanism in disordered conductors can be deduced from the temperature dependence of the conductivity. Under the condition that the carbon black concentration is far above the electrical percolation threshold, $\sigma_{e,ac} \gg \sigma_{i,ac}$, and therefore a plot of σ_{ac} versus temperature should provide some insight into the nature of charge transport in these systems. The temperature dependence of $\sigma_{e,ac}$ for two concentrations of the Ketjen suspensions and one concentration of the Vulcan suspension far above $\phi_{c,e}$ is shown in Figure 4a. The ac conductivity at concentrations above $\phi_{c,e}$ shows an exponential increase of the conductivity with temperature. This behavior is characteristic of a nonmetallic response in semiconductors suggesting the transport process is activated. The generalized Mott equation describes the temperature dependence of the conductivity of a wide variety of disordered semiconductors, $\sigma_{e,ac} = \sigma_0/T^{\beta}\exp(-(T_0/T)^{\alpha})$.[28] The parameters α and β are related to the nature of electron transport. Due to the colloidal nature of these samples, it is anticipated that the variable range hopping (VRH) model will be the correct description where α = 0.25 and β = 0.5 and the hopping takes place from localized states or traps within the conduction band. Fits to the VRH model are overlaid on the experimental data and, for the limited temperature range measured, show good agreement with the model. The Ketjen sample above the gel concentration shows temperature scaling identical to that for both the Ketjen and Vulcan samples below the jamming transition. Consistency with the VRH model requires that the relaxation strength $\Delta\varepsilon = \varepsilon_{20kHz} - \varepsilon_{10MHz}$ decreases with increasing temperature, which is indeed observed for all samples as is shown in Figure 4b.[29] Comparison of the temperature dependence of the conductivity with competing models shown in Supporting Information Figure S.7 confirms that VRH represents the best agreement to these data, but more definitive assignment would require an expanded temperature range.

Structural Connection between Electrical and Mechanical Properties. The Hamaker constant expected for two graphite spheres dispersed in polar solvents can be as high as ~25 k_BT.[30] Ketjen and Vulcan particles do possess a weak surface charge, the ζ potential measured for Vulcan and Ketjen (−20 and −16 mV in neat propylene carbonate, respectively), which is sufficient to resist aggregation at very dilute concentrations. As noted in the DLS measurements, we observe a stable fluid phase composed of only primary aggregates under very dilute conditions, $\phi_{eff} < 0.001$ for both carbon blacks. The colloidal stability of strongly attractive dilute suspensions of colloids has been addressed using mode-coupling theory by Bergenholtz et al. for square-well fluids.[31] With the limits of low volume fraction, $\phi \to 0$, and large well depth, $U \to \infty$, a nonergodicity transition is expected to occur at volume fractions insufficient to form stress-bearing networks. Strong attraction between carbon aggregates is often invoked to explain the gelation behavior of carbon black suspensions. However, our data suggest that gelation does not occur due to the strong attraction between primary aggregates, but instead first a clustered fluid phase forms which then forms the system-spanning network when further concentrated. Recent work has shown that a long-range, weak repulsion can be sufficient to stabilize a reentrant ergodic fluid phase composed of fractal clusters.[2,32] This phase arises due to the renormalization of the pair potential between clusters as they grow. The particles contained within such clusters are trapped and the local

DOI: 10.1021/acs.langmuir.7b02538
Langmuir 2017, 33, 12260−12266

dynamics appear arrested, but the clusters themselves are ergodic and free to diffuse. A reentrant clustered fluid phase is consistent with both the USANS and dynamic light scattering measurements. Above a critical concentration, the aggregation rate becomes finite and cluster formation is favored. As the samples are concentrated further, the cluster number density grows until they form a physically bonded network with a finite modulus. In contrast to gel networks where the attractive bonds between primary colloidal particles form the stress-bearing network, the building blocks of gels formed from reentrant clustered phases are likely weakly attractive or even repulsive. The structural hierarchy provided by this mechanism suggests that gels of carbon black in neat propylene carbonate are comprised of dynamically arrested clusters with many strong bonds within the clusters (intracluster bonds) and a small number of weak bonds between clusters (intercluster bonds). Therefore, the elastic moduli, which indicates the number density and topology of the stress-bearing bonds, are determined primarily by the intercluster bonds. For such a scenario, the topological fractal dimension can be related to the critical rheological exponent via the relation, $D_f = 3 - 1/q$. Using this relationship, $D_f = 2.6$ and 2.7 for Ketjen and Vulcan suspensions, respectively.[33]

This physical picture explains both the microstructural and rheological measurements, but it does not explain the observed electrical properties of these suspensions. Rather, electrical percolation occurs for very low volume fractions as compared with the jamming transition, i.e., $\phi_{c,e} = 0.005$ and 0.01 for Ketjen and Vulcan, respectively. If, as has been hypothesized, the stress-bearing bonds (i.e., the intercluster bonds) are also responsible for conveying electrical charges throughout the sample, then electrical percolation should occur at or near $\phi_{c,g}$ as the number density of these bonds becomes finite. For colloidal suspensions, a finite modulus at zero frequency requires an average bond number of 2.4. The condition, however, for a system-spanning network requires only an average bond number greater than 2.[34] Such string-like particle networks, while sufficient to conduct electrical charge, would not contribute to an elastic stress. While this argument can in principle predict a difference between the electrical and mechanical percolation volume fractions, it fails to explain the evolution of electrical conductivity under shear flow in carbon black suspensions observed in the literature.[35,36] The application of steady shear to such a system should break these tenuous bonds, particularly at high shear rates where the shear stress overcomes the attractive interactions holding the particles together. While the electrical conductivity is generally seen to decrease under such conditions, this decrease is modest and electrical percolation is maintained. This observation has been noted by others who have looked at the evolution of conductivity under shear flow.[9] Therefore, while the elastic bonds that comprise the network may contribute marginal conductivity to the system, they do not dominate the electrical behavior. A similar mechanism has been invoked to explain the thermal conductivity of nanofluids composed of graphite flakes in ethylene glycol where isolated graphite flakes first cluster and then percolate to form a stress-bearing structure. In these systems, it is the localization of solvent into the clustered phase that is responsible for a rapid increase in thermal conductivity over a narrow volume fraction[37] Electrical percolation must, therefore, be independent of the network elasticity. This is allowed because hopping transport does not require intimate mechanical contact between conducting phases for charge transport to occur. Consequently, microstructural reorganization provided by diffusion can bring two conducting phases within the distance necessary for hopping to take place. This is behavior similar to that observed for the percolation of water-in-oil microemulsions, where the conductivity can be described near the percolation threshold by considering a characteristic structural rearrangement time relative to the diffusivity of free charges within a conducting site.[38]

Further insight into the dynamics of the charge transfer process comes from the power-law scaling of the ac conductivity, $\sigma_{e,ac}(\omega) \sim \omega^u$ where $\omega = 2\pi f$ is used in eq S.5 to fit the high-frequency impedance spectroscopy. This behavior is often seen in a wide range of disordered conductors. This scaling, sometimes called a Jonscher power law, generally occurs when charge carriers (be they electrons, ions, polarons, or holes) transport via discrete transitions in localized states.[39] Hopping, trapping, and tunneling process all can give rise to such a dielectric response, and therefore it is seen in a wide range of materials.[40] The dispersive nature of the response indicates a self-similarity (either structural or temporal) that dominates charge transport in these systems. The response can sometimes be associated with a conduction current relaxation that arises due to mobile charge carriers that take part in these transport processes via conduction bands.[41] Both the anomalous and the Debye-like response are present in all concentrations above $\phi_{c,e}$ tested, and the fits of the impedance spectra to eq S.6 support that both types of transport are necessary to describe adequately the frequency dependence.

At high frequency (>10^6 Hz) the parameter u depends on the dynamic nature of charge transfer events. If this high-frequency ac process is connected to the mobile charge dynamics that determine the conduction current relaxation, then, in general, the two responses will follow the same volume fraction dependence. The two responses can be compared using the relationship, $u = t/(s + t)$ where t and s are the critical exponents that define the scaling relations, $\sigma_{e,ac} \sim (\phi_{eff} - \phi_{c,e})^t$ and $\Delta\varepsilon \sim (\phi_{eff} - \phi_{c,e})^s$. In Figure 5, we compare u calculated directly from the high-frequency limit of the conductivity and that determined from $u = t/(s + t)$ where t and s are determined as a function of volume fraction using a derivative method (see the Supporting Information).[42,43] Near the $\phi_{c,e}$, the value of u is very close to that expected at percolation—0.72—shown as the horizontal black dashed line in Figure 5. Beyond the electrical percolation threshold, the critical exponents derived from the two methods show excellent agreement. Using both analyses, the value for u approaches 0.5 as the samples near the $\phi_{c,g}$.[40,44] This analysis shows that the electrical response described by eq S.6 relates to electron motion along the same critical path. Further it shows that this path is not directly linked to the nature of the stress-bearing network but is instead linked to the dynamics of the primary aggregate and cluster motions. As the VRH characteristics are maintained through the $\phi_{c,g}$, this shows that the presence of stress-bearing bonds is not necessary to convey electrons throughout the sample. Further, we postulate that the diffusional motion of the mobile primary aggregates/clusters which determine the distribution of trapping and waiting times determines the magnitude of u. The change of u from 0.72 to 0.5 suggests a continuous transition in electrical properties as these dynamics slow on approach to the gel point. At the gel point, electron transport becomes dominated by the random walk of carriers through the three-dimensional network that comprises the gel, but importantly it is the distribution of cluster/aggregates within the sample that determines the

DOI: 10.1021/acs.langmuir.7b02538
Langmuir 2017, 33, 12260−12266

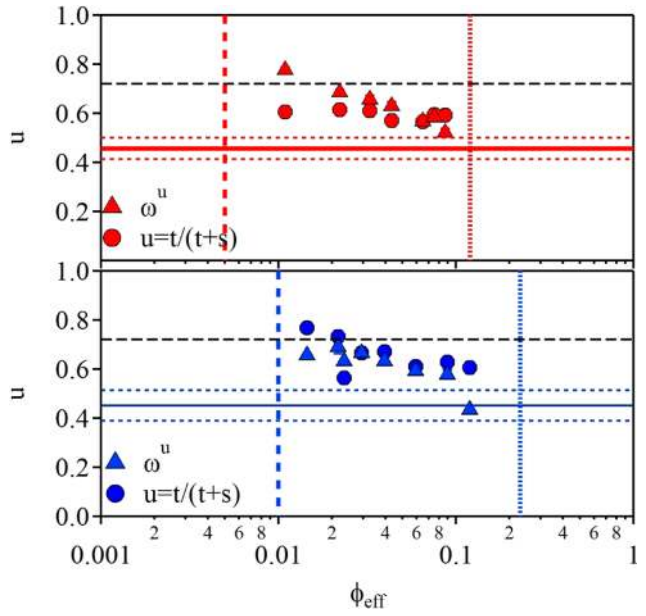

Figure 5. Exponent u determined from the power-law scaling of $\sigma_{e,ac} \sim \omega^u$ and that determined from the scaling of $u = t/(s + t)$ for Ketjen (top) and Vulcan (bottom). The vertical long-dashed line denotes the onset of electrical percolation, and the vertical short-dashed line demarks $\phi_{c,g}$. The horizontal black dashed line marks the value of $u = 0.72$ based on percolation theory,[42] and the horizontal red and blue solid lines are the values for u determined from scaling of the conductivity and permittivity above $\phi_{c,g}$ and the small-dashed lines are the estimated uncertainty of those values.

topology of the percolated path and not the physical connectivity.

CONCLUSIONS

In this work, we combine SANS, oscillatory rheology, and impedance spectroscopy to investigate the relationship between the structural, mechanical, and electrical properties of quiescent carbon black suspensions. The electrical and mechanical percolation thresholds are measured, which shows that the onset of electrical percolation throughout these suspensions occurs well before the gel transitions. Further, hopping is shown to be the dominant charge transport mechanism below and above the gel transitions. Therefore, the stress-bearing chains that provide for a finite elastic modulus are not the dominant contributor to the electrical behavior, and instead, dynamic interactions dominate the variable range hopping mechanism. This is determined both from the temperature dependence of the ac conductivity as well as the volume fraction dependence of the permittivity. Further, the microstructural characterization in this work identifies a double ergodicity breaking mechanism as a function of volume fraction, where first colloidal carbon black aggregates become unstable against aggregation and form a reentrant clustered fluid phase. Upon further concentration, the clustered fluid jams resulting in relatively weak, heterogeneous gel.

These findings help explain several observations for carbon black suspensions present in the literature, including the power-law scaling between the electrical conductivity and elastic moduli. This phenomenon arises because of the heterogeneity of the network determined by the relative distribution of aggregates and clusters, which in turn is a function of the sample's shear history. Further, we assign a different mechanistic understanding to the origin of the electrical and mechanical responses with respect to the prior literature that is supported by a detailed microstructural study. These findings also agree with reports of the shear rate dependent conductivity data for carbon black suspensions; i.e., because direct carbon particle contact is unnecessary to maintain conductive pathways throughout the sample, the application of steady shear does not significantly affect the dominant charge transport mechanism. Rather, shearing affects the cluster size distribution. We speculate that these new insights provide a potential path forward to design lower viscosity conductive additives for electrochemical flow applications as the interactions between carbon black aggregates can be designed to optimize for a cluster size distribution that provides for the maximum conductivity without a corresponding increase in viscosity.

ASSOCIATED CONTENT

Supporting Information

The Supporting Information is available free of charge on the ACS Publications website at DOI: 10.1021/acs.langmuir.7b02538.

Frequency dependent viscoelastic moduli, scattering data and model fits with parameters, impedance spectroscopy data with model fits and description, and temperature dependent ac conductivity model comparison (PDF)

AUTHOR INFORMATION

Corresponding Author

*E-mail: Jeffrey.Richards@nist.gov. Tel.: 301-975-6706.

ORCID

Jeffrey J. Richards: 0000-0003-2173-6204
John K. Riley: 0000-0001-6132-0751
Norman J. Wagner: 0000-0001-9565-619X

Notes

Disclosure: Certain commercial equipment, instruments, or materials are identified in this paper to specify the experimental procedure adequately. Such identification is not intended to imply recommendation or endorsement by the National Institute of Standards and Technology, nor is it intended to imply that the materials or equipment identified are necessarily the best available for the purpose. Unless otherwise specified error bars are one standard deviation from the mean.

The authors declare no competing financial interest.

ACKNOWLEDGMENTS

We acknowledge the NIST Center for Neutron Research CNS Cooperative Agreement No. 70NANB12H239 grant for partial funding as well as the National Research Council for support. This work benefited from the use of the SasView application (Version 4.0), originally developed under NSF Award DMR-0520547. SasView contains code developed with funding from the European Union's Horizon 2020 research and innovation program under the SINE2020 project, Grant Agreement No. 654000.

REFERENCES

(1) Trappe, V.; Prasad, V.; Cipelletti, L.; Segre, P. N.; Weitz, D. A. Jamming Phase Diagram for Attractive Particles. *Nature* **2001**, *411* (6839), 772−775.

(2) Kroy, K.; Cates, M. E.; Poon, W. C. K. Cluster Mode-Coupling Approach to Weak Gelation in Attractive Colloids. *Phys. Rev. Lett.* **2004**, *92* (14), 148302.

DOI: 10.1021/acs.langmuir.7b02538
Langmuir 2017, 33, 12260−12266

(3) Pham, K. N.; Petekidis, G.; Vlassopoulos, D.; Egelhaaf, S. U.; Poon, W. C. K.; Pusey, P. N. Yielding Behavior of Repulsion- and Attraction-Dominated Colloidal Glasses. *J. Rheol.* **2008**, *52* (2008), 649.
(4) Duduta, M.; Ho, B.; Wood, V. C.; Limthongkul, P.; Brunini, V. E.; Carter, W. C.; Chiang, Y. M. Semi-Solid Lithium Rechargeable Flow Battery. *Adv. Energy Mater.* **2011**, *1* (4), 511−516.
(5) Dennison, C. R.; Beidaghi, M.; Hatzell, K. B.; Campos, J. W.; Gogotsi, Y.; Kumbur, E. C. Effects of Flow Cell Design on Charge Percolation and Storage in the Carbon Slurry Electrodes of Electrochemical Flow Capacitors. *J. Power Sources* **2014**, *247*, 489−496.
(6) Hatzell, K. B.; Beidaghi, M.; Campos, J. W.; Dennison, C. R.; Kumbur, E. C.; Gogotsi, Y. A High Performance Pseudocapacitive Suspension Electrode for the Electrochemical Flow Capacitor. *Electrochim. Acta* **2013**, *111*, 888−897.
(7) Smith, K. C.; Chiang, Y.-M.; Craig Carter, W. Maximizing Energetic Efficiency in Flow Batteries Utilizing Non-Newtonian Fluids. *J. Electrochem. Soc.* **2014**, *161* (4), A486−A496.
(8) Helal, A.; Divoux, T.; McKinley, G. H. Simultaneous Rheoelectric Measurements of Strongly Conductive Complex Fluids. *Phys. Rev. Appl.* **2016**, *6* (6), 064004.
(9) Narayanan, A.; Mugele, F.; Duits, M. H. G. Mechanical History Dependence in Carbon Black Suspensions for Flow Batteries: A Rheo-Impedance Study. *Langmuir* **2017**, *33* (7), 1629−1638.
(10) Dullaert, K.; Mewis, J. A Structural Kinetics Model for Thixotropy. *J. Non-Newtonian Fluid Mech.* **2006**, *139* (1−2), 21−30.
(11) Kline, S. R. Reduction and Analysis of SANS and USANS Data Using IGOR Pro. *J. Appl. Crystallogr.* **2006**, *39* (6), 895−900.
(12) Hollingsworth, A. D.; Saville, D. A. Dielectric Spectroscopy and Electrophoretic Mobility Measurements Interpreted with the Standard Electrokinetic Model. *J. Colloid Interface Sci.* **2004**, *272* (1), 235−245.
(13) Hollingsworth, A. D.; Saville, D. A. A Broad Frequency Range Dielectric Spectrometer for Colloidal Suspensions: Cell Design, Calibration, and Validation. *J. Colloid Interface Sci.* **2003**, *257* (1), 65−76.
(14) Liu, A. J.; Nagel, S. R. Nonlinear Dynamics: Jamming Is Not Just Cool Any More. *Nature* **1998**, *396* (6706), 21−22.
(15) Ehrburger-Dolle, F.; Lahaye, J.; Misono, S. Percolation in Carbon Black Powders. *Carbon* **1994**, *32* (7), 1363−1368.
(16) Lu, P. J.; Zaccarelli, E.; Ciulla, F.; Schofield, A. B.; Sciortino, F.; Weitz, D. A. Gelation of Particles with Short-Range Attraction. *Nature* **2008**, *453* (7194), 499−503.
(17) Richards, J. J.; Gagnon, C. V. L; Krzywon, J. R.; Wagner, N. J.; Butler, P. D. Dielectric RheoSANS-Simultaneous Interrogation of Impedance, Rheology and Small Angle Neutron Scattering of Complex Fluids. *J. Visualized Exp.* **2017**, No. 122, e55318.
(18) Pedersen, J. S. Analysis of Small-Angle Scattering Data from Colloids and Polymer Solutions: Modeling and Least-Squares Fitting. *Adv. Colloid Interface Sci.* **1997**, *70*, 171−210.
(19) Cates, M. E.; Wittmer, J. P.; Bouchaud, J.-P.; Claudin, P. Jamming, Force Chains, and Fragile Matter. *Phys. Rev. Lett.* **1998**, *81* (9), 1841−1844.
(20) Stradner, A.; Sedgwick, H.; Cardinaux, F.; Poon, W. C. K.; Egelhaaf, S. U.; Schurtenberger, P. Equilibrium Cluster Formation in Concentrated Protein Solutions and Colloids. *Nature* **2004**, *432* (7016), 492−495.
(21) Sciortino, F.; Mossa, S.; Zaccarelli, E.; Tartaglia, P. Equilibrium Cluster Phases and Low-Density Arrested Disordered States: The Role of Short-Range Attraction and Long-Range Repulsion. *Phys. Rev. Lett.* **2004**, *93* (5), 055701.
(22) Hartley, P. a; Parfitt, G. D. Dispersion of Powders in Liquids. 1. The Contribution of the van Der Waals Force to the Cohesiveness of Carbon Black Powders. *Langmuir* **1985**, *1*, 651−657.
(23) Osuji, C. O.; Kim, C.; Weitz, D. A. Shear Thickening and Scaling of the Elastic Modulus in a Fractal Colloidal System with Attractive Interactions. *Phys. Rev. E* **2008**, *77* (6), 060402.
(24) Richards, J. J.; Scherbarth, A. D.; Wagner, N. J.; Butler, P. D. Mixed Ionic/Electronic Conducting Surface Layers Adsorbed on Colloidal Silica for Flow Battery Applications. *ACS Appl. Mater. Interfaces* **2016**, *8* (36), 24089−24096.
(25) Ambrosetti, G.; Grimaldi, C.; Balberg, I.; Maeder, T.; Danani, A.; Ryser, P. Solution of the Tunneling-Percolation Problem in the Nanocomposite Regime. *Phys. Rev. B: Condens. Matter Mater. Phys.* **2010**, *81* (15), 155434.
(26) Nuzhnyy, D.; Savinov, M.; Bovtun, V.; Kempa, M.; Petzelt, J.; Mayoral, B.; McNally, T. Broad-Band Conductivity and Dielectric Spectroscopy of Composites of Multiwalled Carbon Nanotubes and Poly(ethylene Terephthalate) around Their Low Percolation Threshold. *Nanotechnology* **2013**, *24* (5), 055707.
(27) Pelster, R.; Simon, U. Nanodispersions of Conducting Particles: Preparation, Microstructure and Dielectric Properties. *Colloid Polym. Sci.* **1999**, *277* (1), 2−14.
(28) Capaccioli, S.; Lucchesi, M.; Rolla, P. a; Ruggeri, G. Dielectric Response Analysis of a Conducting Polymer Dominated by the Hopping Charge Transport. *J. Phys.: Condens. Matter* **1998**, *10*, 5595−5617.
(29) Singh, R.; Kumar, J.; Singh, R. K.; Rastogi, R. C.; Kumar, V. Low Frequency Ac Conduction and Dielectric Relaxation in Pristine poly(3-Octylthiophene) Films. *New J. Phys.* **2007**, *9* (4007), 40−1367.
(30) Dagastine, R. R.; Prieve, D. C.; White, L. R. Calculations of van Der Waals Forces in 2-Dimensionally Anisotropic Materials and Its Application to Carbon Black. *J. Colloid Interface Sci.* **2002**, *249* (1), 78−83.
(31) Bergenholtz, J.; Fuchs, M.; Voigtmann, T. Colloidal Gelation and Non-Ergodicity Transitions. *J. Phys.: Condens. Matter* **2000**, *12* (29), 6575−6583.
(32) Lu, P. J.; Conrad, J. C.; Wyss, H. M.; Schofield, A. B.; Weitz, D. A. Fluids of Clusters in Attractive Colloids. *Phys. Rev. Lett.* **2006**, *96* (2), 028306.
(33) Shih, W.-H.; Shih, W. Y.; Kim, S.-I.; Liu, J.; Aksay, I. A. Scaling Behavior of the Elastic Properties of Colloidal Gels. *Phys. Rev. A: At., Mol., Opt. Phys.* **1990**, *42* (8), 4772−4779.
(34) Valadez-Perez, N. E.; Liu, Y.; Eberle, A. P. R.; Wagner, N. J.; Castaneda-Priego, R. Dynamical Arrest in Adhesive Hard-Sphere Dispersions Driven by Rigidity Percolation. *Phys. Rev. E* **2013**, *88* (6), 060302.
(35) Youssry, M.; Madec, L.; Soudan, P.; Cerbelaud, M.; Guyomard, D.; Lestriez, B. Non-Aqueous Carbon Black Suspensions for Lithium-Based Redox Flow Batteries: Rheology and Simultaneous Rheo-Electrical Behavior. *Phys. Chem. Chem. Phys.* **2013**, *15* (34), 14476−14486.
(36) Mewis, J.; de Groot, L. M.; Helsen, J. A. Dielectric Behaviour of Flowing Thixotropic Suspensions. *Colloids Surf.* **1987**, *22* (2), 271−289.
(37) Zheng, R.; Gao, J.; Wang, J.; Feng, S. P.; Ohtani, H.; Wang, J.; Chen, G. Thermal Percolation in Stable Graphite Suspensions. *Nano Lett.* **2012**, *12* (1), 188−192.
(38) Chen, S. H.; Rouch, J.; Sciortino, F.; Tartaglia, P. Cluster Description of Water-in-Oil Microemulsions near the Critical and Percolation Points. *Nuovo Cimento Soc. Ital. Fis., D* **1994**, *16* (9), 1419−1431.
(39) Jonscher, A. K. Electronic Properties of Amorphous Dielectric Films. *Thin Solid Films* **1967**, *1* (3), 213−234.
(40) Dissado, L. A.; Hill, R. M. Anomalous Low-Frequency Dispersion. Near Direct Current Conductivity in Disordered Low-Dimensional Materials. *J. Chem. Soc., Faraday Trans. 2* **1984**, *80* (3), 291.
(41) Niklasson, G. A. Comparison of Dielectric Response Functions for Conducting Materials. *J. Appl. Phys.* **1989**, *66*, 4350−4359.
(42) Niklasson, G. A. Fractal Aspects of the Dielectric Response of Charge Carriers in Disordered Materials. *J. Appl. Phys.* **1987**, *62* (7), R1−R14.
(43) Gefen, Y.; Aharony, A.; Alexander, S. Anomalous Diffusion on Percolating Clusters. *Phys. Rev. Lett.* **1983**, *50* (1), 77−80.
(44) Dissado, L. A.; Hill, R. M. The Fractal Nature of the Cluster Model Dielectric Response Functions. *J. Appl. Phys.* **1989**, *66* (6), 2511−2524.

DOI: 10.1021/acs.langmuir.7b02538
Langmuir 2017, 33, 12260−12266